Lab on a Chip

PAPER

Rapid discrimination of DNA strands using an opto-calorimetric microcantilever sensor†

Dongkyu Lee,*[a] Kyo Seon Hwang,*[b] Seonghwan Kim[c] and Thomas Thundat[a]

Cite this: *Lab Chip*, 2014, **14**, 4659

Received 28th August 2014,
Accepted 23rd September 2014

DOI: 10.1039/c4lc01000k

www.rsc.org/loc

A rapid technique for quantitative detection and discrimination of DNA strands without using immobilized probe molecules is demonstrated using an opto-calorimetric, self-powered sensor based on a $Pb(Zr_{0.52}Ti_{0.48})O_3$ (PZT) microcantilever. Microcalorimetric infrared (IR) spectroscopy provides excellent chemical selectivity based on the unique molecular vibrational characteristics of each nucleotide in the mid IR region. The piezoelectric and pyroelectric properties of the PZT microcantilever were exploited in the quantitative detection and discrimination of adsorbed DNA strands with their spectral characteristics. We report the unique spectral characteristics of different DNA nucleotides that are monitored by wavelength-dependent temperature variations for different relative molar ratio of each nucleotide. This approach offers a fast, label-free technique which is highly sensitive and selective for the detection of single nucleotide differences in DNA strands and has the potential to be used as a rapid prescreening biosensor for various biomolecules.

Introduction

Microfabricated sensors such as microcantilevers, microbridges, and micromembranes have attracted much attention as effective label-free biosensing platforms due to their extremely high sensitivity, small size, and multiplexing capability. These sensors have been used in the detection of biomolecular interactions such as DNA hybridization and receptor–ligand binding.[1–4] However, immobilized probe molecule-based biosensors have several issues such as unspecific binding of unsought molecules and non-uniform immobilization coverage which leads to large variations in sensor responses. Despite the intrinsic selectivity of biological interactions between probe and target molecules, there continue to be issues with reproducibility of results. Furthermore, the multiple steps involved in immobilizing probe molecules, the time-consuming analyte delivery process, and the reaction time between probe and target molecules impose severe limitations on microfabricated biosensors for the rapid and facile detection of biomolecules. To overcome these problems, different immobilization-free sensing techniques such as optical spectroscopy, electrochemical methods, labeling and particle-assisted methods have been demonstrated.[5–9] However, these techniques usually require additional steps and tedious calibrations for quantitative detection of biological analytes. Although conventional optical spectroscopic techniques such as Fourier transform infrared (FTIR) and Raman spectroscopy have excellent selectivity for molecular detection, they suffer from low sensitivity, challenges in quantitative measurements and miniaturization.

Among various sensing techniques, microcalorimetric infrared (IR) spectroscopy based on a bimetallic microcantilever has offered rapid molecular identification with high selectivity and sensitivity since it combines the sensitivity of a thermomechanical sensor and the selectivity of IR spectroscopy without the need for labels or the immobilization of probe molecules.[10–12] The absorption of IR radiation by molecules adsorbed on the microcantilever results in a small variation in the cantilever temperature depending on the IR absorption characteristics of the molecules. Then, this minute temperature variation as a function of illuminating IR wavelength is sensitively transduced as nanomechanical deflection of the bimetallic microcantilever resulting in nanomechanical IR spectra. Furthermore, resonance frequency shifts of the cantilever enable the determination of the adsorbed mass of target molecules making this technique quantitative. This multi-modal sensing method allows quantitative molecular recognition with minimal calibration.[13]

Lead zirconate titanate, $Pb(Zr_{0.52}Ti_{0.48})O_3$, (PZT) film has been utilized as a base material in piezoelectric actuators[14]

[a] *Department of Chemical and Materials Engineering, University of Alberta, Edmonton, AB T6G 2V4, Canada. E-mail: dongkyu@ualberta.ca; Tel: +1780 492 8763*
[b] *Center for BioMicrosystems, Brain Science Institute, Korea Institute of Science and Technology, Seoul, South Korea. E-mail: kshwang@kist.re.kr; Tel: +82 2 958 6727*
[c] *Department of Mechanical and Manufacturing Engineering, University of Calgary, Calgary, AB T2N 1N4, Canada*

† Electronic supplementary information (ESI) available. See DOI: 10.1039/c4lc01000k

or pyroelectric uncooled IR detectors.[15–17] Contrary to other uncooled IR detectors, the PZT film-embedded microcantilever in this study is exploited as both a highly sensitive resonator and a self-powered calorimetric sensor. This novel approach utilizes both the piezoelectric and pyroelectric properties of the PZT film in a single device. Frequency responses as well as thermal responses of the PZT cantilever are sensitively measured with an electrical readout scheme, which eliminates conventional optical lever readout components. Here, we demonstrate a rapid and facile prescreening technique for DNA and single nucleotide difference (SND) without the need for immobilized probe molecules. The selective detection of DNA with multiple nucleotides and rapid screening of SNDs are enabled by analyzing variations in the profile of calorimetric IR spectra due to the different relative molar ratio of individual nucleotides.

Experiments

PZT microcantilevers

Microfabrication processes of PZT monolithic microcantilevers were reported in our previous publication.[14] The microcantilever with an embedded piezoelectric thin film was composed of six multilayers, SiN_x/Ta/Pt/PZT/Pt/SiO_2, having a total thickness of 2.18 μm, in order to achieve a simple self-actuating and self-powered heat sensing. A PZT film with a thickness of 0.7 μm was deposited using a sol–gel process. The thin layers of platinum deposited on the PZT film served as electrodes. The remnant polarization value of the PZT thin film in the microcantilever structure was approximately 15 μC cm^{-2} at room temperature when a 100 kV cm^{-1} electric field was used to induce polarization. Each PZT cantilever was 300 μm long and 100 μm wide with a spring constant of ~1.48 N m^{-1} as shown in Fig. 1.

DNA samples

We used synthetic single-stranded DNA (ssDNA) with 20 bases of adenine (A_{20}), thymine (T_{20}), cytosine (C_{20}), and guanine (G_{20}) for the reference spectra of each nucleotide. Various ssDNA strands with complex nucleotides and one different nucleotide were used to demonstrate the proof-of-concept experiments (ATGC: 5′-ATG CAT GCA TGC ATG CAT GC-3′, ACTTCA: 5′-ACT TCA ACT TCA ACT TCA AC-3′, ACTCCA: 5′-ACT TCA ACT CCA ACT TCA AC-3′, GTTGAA: 5′-GTT GAA GTT GAA GTT GAA GT-3′). The initial concentration of each ssDNA solution was 10 μM in deionized water. The solution was deposited on the cantilever by inserting the cantilever into a microglass capillary containing the DNA solution and slowly taking the cantilever out of the capillary.

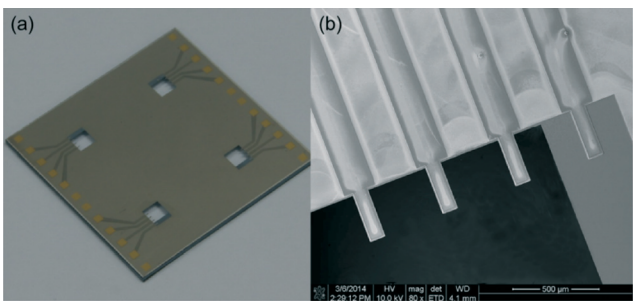

Fig. 1 (a) Optical image of the PZT microcantilever array chip and (b) SEM image of PZT microcantilevers.

Experimental setup

Fig. 2(a) shows the schematic illustration of the experimental setup. The 100 kHz pulsed IR radiation with 5% duty cycle from a quantum cascade laser (QCL) (Daylight Solutions, San Diego, CA) was electrically burst at 40 Hz using a DS345 function generator (Stanford Research Systems, Sunnyvale, CA), and the pulsed IR was illuminated onto the cantilever. The IR wavelength was scanned in a wavenumber range of 1760 cm^{-1} to 1565 cm^{-1} with a step size of 1.4 cm^{-1}. The calorimetric IR spectra were collected without any signal amplification by connecting the cantilever to an SR850 lock-in amplifier (Stanford Research Systems). The resonance frequencies of the cantilever, which can be exploited to determine the adsorbed mass of ssDNAs, were monitored before and after the deposition of ssDNAs using the same lock-in amplifier. This technique provides two orthogonal signals in a single transducer platform from both pyroelectric and piezoelectric properties of the PZT microcantilever, as shown in Fig. 2(b) and (c), used in the quantitative determination of adsorbed DNA mass and their spectral characteristics. The phonons generated by the nonradiative decay process heat the cantilever at a specific IR wavelength which can be observed as variations in the voltage generated by the cantilever. The microcalorimetric IR spectrum can be obtained by a

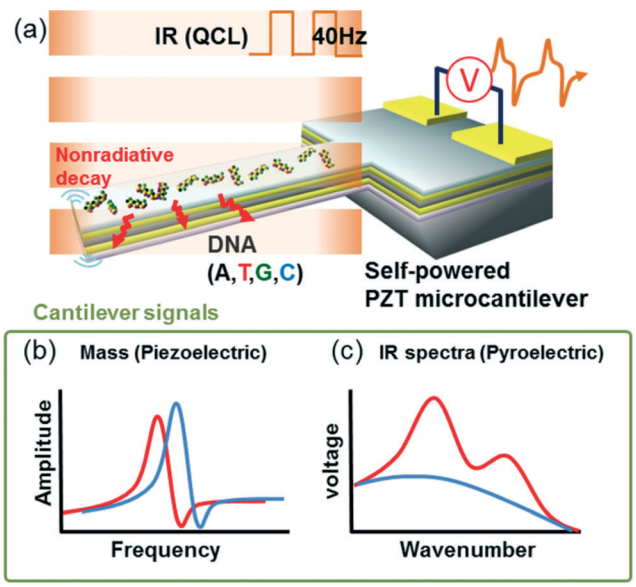

Fig. 2 (a) Schematic illustration of a self-powered calorimetric IR spectrometer based on the PZT microcantilever. Schematic illustration of variations in the resonance frequency (b) and the microcalorimetric IR spectra (c) of the PZT microcantilever without (blue) and with target molecules (red) from its piezoelectric as well as pyroelectric properties.

differential plot of the amplitude of the voltage generation as a function of IR wavenumber with and without target molecules.

FTIR microscopy

Various ssDNA strands on gold-coated silicon were characterized using a standard FTIR technique as references. 10 microliters of 10 μM ssDNA solution was drop-cast onto the gold-coated silicon substrate. The surface density of ssDNA molecules onto gold-coated silicon was 10 times higher than that onto the PZT microcantilever (approximately ~100 μg cm^{-2}). FTIR spectra were obtained using an FTIR microscope (Nicolet Continuμm™, Thermo Scientific) in reflection mode. The number of registered scans was 200 with a resolution of 1 cm^{-1}.

Results and discussion

The PZT microcantilever serves as an extremely sensitive pyroelectric heat sensor as well as a piezoelectric microresonator for the detection, speciation, and quantification of adsorbed ssDNAs. Fig. 3(a) shows the variations in the resonance frequency of the PZT microcantilever when A_{20} was adsorbed on the cantilever. Assuming that the ssDNA molecules are evenly adsorbed on the cantilever surface and do not affect the stiffness of the cantilever, the adsorbed mass of the ssDNA can be calculated with the following equation.

$$\Delta m = 2m_0 \frac{\Delta f}{f_0} \quad (1)$$

where Δm is the mass of the adsorbate, m_0 is the mass of the clean cantilever, Δf is the change in the resonance frequency of the cantilever, and f_0 is the initial resonance frequency of the clean cantilever. The dark yellow line in Fig. 3(a) is the initial resonance frequency. The adsorbed mass of A_{20} on the PZT microcantilever was determined to be in the range of ~0.1 ng to 4 ng. The resonance frequency decreased more as the adsorbed mass increased (0.1 ng (black), 0.49 ng (red), 1.2 ng (green), and 4 ng (blue)). Fig. 3(b) shows the microcalorimetric IR spectra with respect to the adsorbed mass of A_{20}. The major peaks at 1661 cm^{-1} and 1607 cm^{-1} in adenine correspond to NH_2 bending mode and ring bond C═C, C═N stretching vibration, respectively. The inset shows a magnified view of the spectra with the adsorbed mass of 0.1 ng and 0.49 ng. All of the spectral data are presented as raw data without any signal processing or smoothing. Fig. 3(c) shows the peak amplitudes at 1661 cm^{-1} in the microcalorimetric IR spectra as a function of the adsorbed mass of A_{20}. The intensity of the peak is directly proportional to the adsorbed mass. The limit of detection (LOD) for A_{20} was estimated to be approximately 47 pg at 1661 cm^{-1} as the straight line intersects with the dashed line. The number of A_{20} at the LOD was calculated to be approximately 1.8×10^7 molecules. However, the LOD of each nucleotide may be varied due to the different spectral intensity of molecular vibration characteristics. The

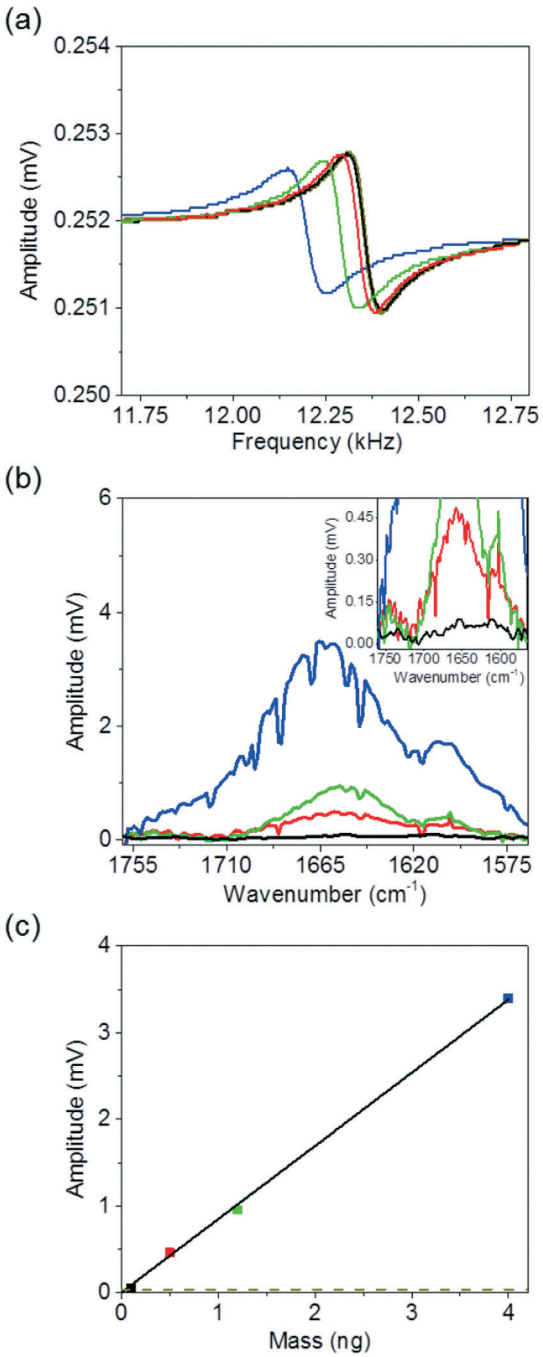

Fig. 3 (a) Variations of the resonance frequency and (b) the microcalorimetric IR spectra of the PZT microcantilever with respect to various adsorbed masses of A_{20} (0.1 ng (black), 0.49 ng (red), 1.2 ng (green), and 4 ng (blue)). The inset of (b) is a magnified view of the spectra of 0.1 ng and 0.49 ng A_{20}. (c) The peak amplitudes at 1661 cm^{-1} as a function of adsorbed mass of A_{20}. The straight line is the linear fit of the peak amplitudes and the dashed line is the minimum peak amplitude for A_{20} with a signal-to-noise ratio of 3.

LOD could be enhanced by increasing the IR laser power or the optimization of pyroelectricity.

Fig. 4(b) shows the normalized microcalorimetric IR absorption spectra of each nucleotide (A_{20}, T_{20}, G_{20}, and C_{20}). The IR spectra of each nucleotide were acquired separately as

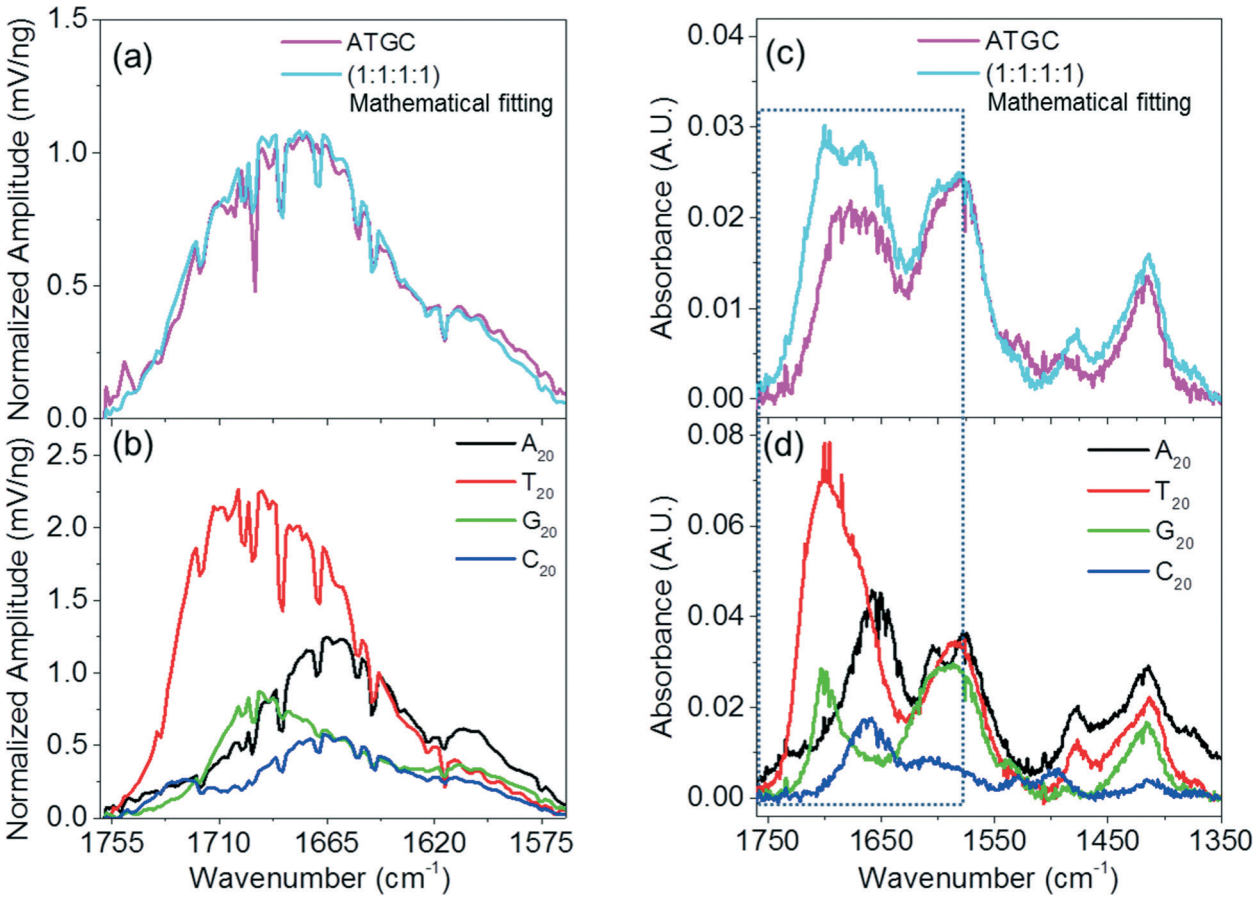

Fig. 4 (a) Normalized calorimetric IR absorption spectrum of ATGC (magenta) and a weighted linear superposition (sky blue) of individual normalized calorimetric IR spectra (A_{20}, T_{20}, G_{20}, and C_{20}). (b) Normalized calorimetric IR absorption spectra of each nucleotide (A_{20} (black), T_{20} (red), G_{20} (green), and C_{20} (blue)). (c) FTIR spectrum of ATGC (magenta) and a weighted linear superposition (sky blue) of individual FTIR spectra (A_{20}, T_{20}, G_{20}, and C_{20}). The dashed square represents the dynamic range of the microcalorimetric IR spectra. (d) Conventional FTIR spectra of each nucleotide (A_{20} (black), T_{20} (red), G_{20} (green), and C_{20} (blue)).

references and were consistent with previously reported results.[18–20] The adsorbed masses of A_{20}, T_{20}, G_{20}, and C_{20} on the cantilever were approximately 4.02 ng, 3.44 ng, 3.72 ng, and 3.16 ng, respectively, calculated using eqn (1). The normalized microcalorimetric IR spectra were obtained by dividing the amplitude of lock-in voltage generation by the mass of adsorbed molecules. The peaks in individual spectra of each nucleotide can be identified as NH_2 bending mode (1661 cm^{-1}) and ring bond C═C, C═N stretching vibration (1607 cm^{-1}) in adenine; carbonyl C═O displacement (1718 cm^{-1} and 1709 cm^{-1}) and N–H bending mode (1661 cm^{-1}), and ring bond C═C stretching vibration (1607 cm^{-1}) in thymine; carbonyl C═O displacement (1694 cm^{-1}) and ring bond C═N stretching (1607 cm^{-1}) in guanine; and carbonyl C═O displacement (1724 cm^{-1} and 1666 cm^{-1}) and ring bond C═C, C═N stretching (1607 cm^{-1}) in cytosine.[19] The different amplitudes of individual spectra were attributed to different intensities of certain characteristic peaks. In addition, it is worth noting that the peaks near 1600–1565 cm^{-1} in the microcalorimetric IR spectra are not clear because of the low power intensity of QCL in this spectral range. These spectra clearly indicate that different bases have specific signatures which result in unique profiles for each spectrum. Fig. 4(a) shows the normalized calorimetric IR absorption spectra of ATGC and a weighted linear superposition of the individual nucleotide spectra. The adsorbed mass of ATGC on the cantilever was approximately 2.2 ng. The relative component ratio (A : T : G : C) of ATGC is 1 : 1 : 1 : 1, which acts as a quaternary mixture. Within a narrow dynamic range, the broad peaks and shoulders observed in the spectrum of ATGC are due to the convolution of individual nucleotide peaks. Comparing the peaks in the spectrum of ATGC with those in the spectrum of individual nucleotides, the peaks between 1760 cm^{-1} and 1565 cm^{-1} are from the stretching vibration of the carbonyl (C═O), amino groups (NH_2, N–H) and ring bonds (C═C, C═N) in nucleotides. The IR spectrum of ATGC can be fitted to the average spectra of individual nucleotides with the relative component ratio. The IR spectrum of ATGC shows excellent agreement with the mathematical fitting to the normalized IR spectra of individual nucleotides since the IR spectrum of the mixture is a linear superposition of individual spectra.

Fig. 4(c) and (d) show the conventional FTIR spectra of each nucleotide (A_{20}, T_{20}, G_{20}, and C_{20}), ATGC, and a weighted

linear superposition of the individual nucleotide spectrum. The peak positions and profiles in the microcalorimetric IR spectra of ssDNA strands in Fig. 4(a) and (b) agree quite well with those in the FTIR spectra. However, the FTIR spectrum of ATGC did not match with the weighted linear superposition by the FTIR spectra of individual nucleotides because of the inhomogeneity in surface concentration, as shown in Fig. 4(c). The variation in the surface density of the molecules induced the different amplitude of the FTIR spectrum even in the same nucleotide (see the ESI†). Therefore, it is very difficult to quantify the IR spectra of DNA with mixed nucleotides from the FTIR spectra of the individual nucleotides. However, our microcalorimetric technique provides the quantitative IR spectra resulting from the measurement of the adsorbed mass on the specific surface area.

To demonstrate whether this method is capable of distinguishing different components of nucleotides and SNDs in a given DNA strand, microcalorimetric IR spectra of various DNA strands on the PZT microcantilevers were collected. Fig. 5 shows the normalized calorimetric IR spectra of three different strands (GTTGAA, ACTTCA, and ACTCCA). The adsorbed masses of GTTGAA, ACTTCA, and ACTCCA on the cantilever were approximately 2.12 ng, 1.62 ng, and 2.06 ng, respectively. Different profiles of the normalized IR spectra in Fig. 5(a) are mainly attributed to the different ratio between guanine and cytosine. GTTGAA is composed of $A_6T_7G_7$, whereas ACTTCA is composed of $A_7T_6C_7$. The dominant peaks in the profiles of the strands were induced by carbonyl C═O displacement (1694 cm^{-1}) in guanine and carbonyl C═O displacement (1724 cm^{-1} and 1666 cm^{-1}) in cytosine. Fig. 5(b) shows the normalized IR spectra of SND between ACTTCA and ACTCCA. ACTTCA is composed of $A_7T_6C_7$, whereas ACTCCA is composed of $A_7T_5C_8$. Even though the difference in the ssDNA was only a single nucleotide, the normalized IR spectra of ACTTCA and ACTCCA were highly distinguishable. The dominant peaks in the profiles of these strands were due to carbonyl C═O displacement (1718 cm^{-1} and 1709 cm^{-1}) and N–H bending mode (1661 cm^{-1}) in thymine and carbonyl C═O displacement (1724 cm^{-1} and 1666 cm^{-1}) in cytosine. The IR spectra of GTTGAA, ACTTCA, and ACTCCA fit very well with the data obtained using a combination of individual spectra of nucleotides following the linear superposition principle (see the ESI†).

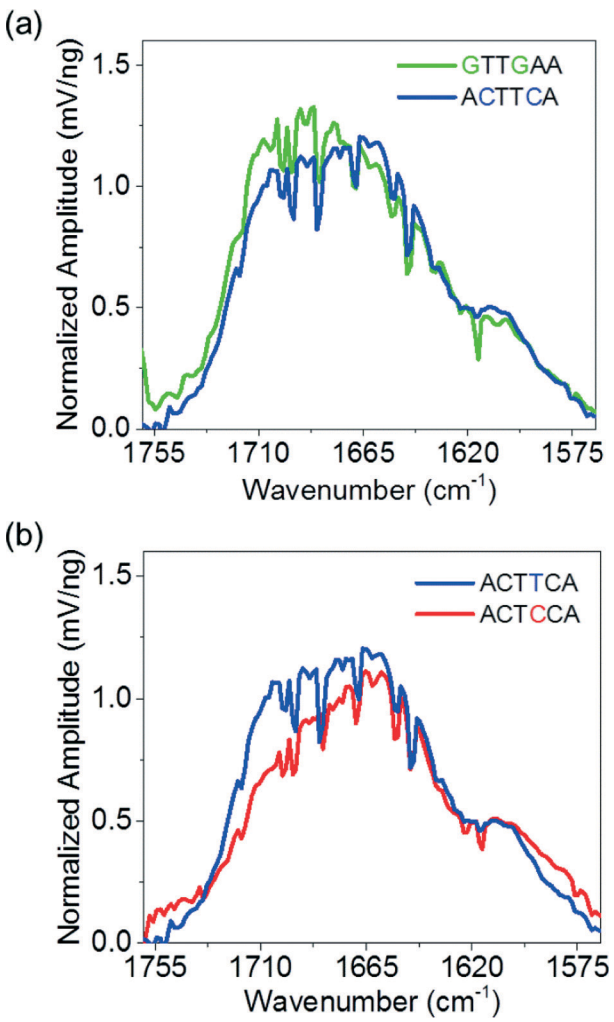

Fig. 5 Normalized microcalorimetric IR absorption spectra of (a) one different component (GTTGAA (green) *vs.* ACTTCA (blue)) and (b) SND (ACTTCA (blue) *vs.* ACTCCA (red)).

This technique is highly sensitive and extremely selective for detecting SNDs in DNA strands and may have potential for use as a rapid prescreening biosensor for various biomolecules. We infer the limit of recognition (LOR) as SND per 30 bases of each nucleotide.[13] However, the LOR of the SND related to adenine and cytosine will be less than that related to other nucleotides due to their similar peaks and profiles in this narrow dynamic range. The LOR can be enhanced by obtaining IR spectra in a wider range, as shown in Fig. 4(c) and (d). Peak positions and intensities between adenine and cytosine are distinguished between 1500 cm^{-1} and 1350 cm^{-1} due to different vibrational displacements (NH_2, imidazole ring, and N═CH deformations at 1470 cm^{-1}, 1453 cm^{-1}, and 1420 cm^{-1}). Although this technique is not able to discern different DNA sequences, it is highly useful as a rapid screening method for potential variations or mutations in a given DNA strand with a known sequence as well as in the detection of conjugation and by-products of biomolecular interactions.[18–21] In addition, it will be a powerful technique when combined with polymerase chain reaction and hybridization-assisted reactions. This technique may also find forensic applications where the need is to discriminate DNA rather than to sequence it and other sensing applications to detect chemical or biological threats.[22]

Conclusions

In summary, we have demonstrated a facile, rapid, and quantitative detection of DNA and screening of SND using immobilization-free, self-powered PZT microcantilevers. Microcalorimetric IR spectroscopy based on a PZT microcantilever offers excellent selectivity due to the unique molecular vibrational spectra of individual nucleotides in the mid IR region which can be

monitored using the pyroelectric properties of a PZT thin film. In addition, this technique is extremely quantitative as adsorbed masses on the PZT cantilever can be monitored piezoelectrically. The screening of SNDs and determination of relative molar ratios on individual nucleotides in DNA strands using normalized calorimetric IR spectra show that this technique is quantitative as well as specific for prescreening applications compared to conventional FTIR instrumentation.

Acknowledgements

D.L. and T.T. would like to acknowledge support from the Canada Excellence Research Chairs (CERC) Program. K.S.H. is very grateful for financial support from the KIST institutional program (2E24590). S.K. acknowledges support from the Schulich School of Engineering at the University of Calgary.

Notes and references

1 G. Wu, R. H. Datar, K. M. Hansen, T. Thundat, R. J. Cote and A. Majumdar, *Nat. Biotechnol.*, 2001, **19**, 856–860.
2 K. M. Hansen, H. F. Ji, G. Wu, R. Datar, R. Cote, A. Majumdar and T. Thundat, *Anal. Chem.*, 2001, **73**, 1567–1571.
3 J. Zhang, H. P. Lang, F. Huber, A. Bietsch, W. Grange, U. Certa, R. Mckendry, H.-J. Guntherodt, M. Hegner and C. Gerber, *Nat. Nanotechnol.*, 2006, **1**, 214–220.
4 J. Fritz, M. K. Baller, H. P. Lang, H. Rothuizen, P. Vettiger, E. Meyer, H. J. Guntherodt, C. Gerber and J. K. Gimzewski, *Science*, 2000, **288**, 316–318.
5 A. T. Krummel and M. T. Zanni, *J. Phys. Chem. B*, 2006, **110**, 13991–14000.
6 X. Luo, T. M. H. Lee and I. M. Hsing, *Anal. Chem.*, 2008, **80**, 7341–7346.
7 X. Luo and I. Hsing, *Biosens. Bioelectron.*, 2009, **25**, 803–808.
8 J.-W. Park, R. Tatavarty, D. W. Kim, H.-T. Jung and M. B. Gu, *Chem. Commun.*, 2012, **48**, 2071–2073.
9 D. Kwon, J. Joo, S. Lee and S. Jeon, *Anal. Chem.*, 2013, **85**, 12134–12137.
10 P. G. Datskos, S. Rajic, M. J. Sepaniak, N. Lavrik, C. A. Tipple, L. R. Senesac and I. Datskou, *J. Vac. Sci. Technol., B: Microelectron. Nanometer Struct.–Process., Meas., Phenom.*, 2001, **19**, 1173–1179.
11 E. T. Arakawa, N. V. Lavrik, S. Rajic and P. G. Datskos, *Ultramicroscopy*, 2003, **97**, 459–465.
12 A. Wig, E. T. Arakawa, A. Passian, T. L. Ferrell and T. Thundat, *Sens. Actuators, B*, 2006, **114**, 206–211.
13 S. Kim, D. Lee, X. Liu, C. V. Neste, S. Jeon and T. Thundat, *Sci. Rep.*, 2013, **3**, 1111.
14 J. H. Lee, K. S. Hwang, J. Park, K. H. Yoon, D. S. Yoon and T. S. Kim, *Biosens. Bioelectron.*, 2005, **20**, 2157–2162.
15 G. De Cicco, B. Morten, D. Dalmonego and M. Prudenziati, *Sens. Actuators, A*, 1999, **76**, 409–415.
16 P. Muralt, *Rep. Prog. Phys.*, 2001, **64**, 1339–1388.
17 B. Bhatia, J. Karthik, T. Tong, D. G. Cahill, L. W. Martin and W. P. King, *J. Appl. Phys.*, 2012, **112**, 104106.
18 A. P. White and J. W. Powell, *Biochemistry*, 1995, **34**, 1137–1142.
19 G. I. Dovbeshko, N. Y. Gridina, E. B. Kruglova and O. P. Pashchuk, *Talanta*, 2000, **53**, 233–246.
20 E. Mateo-Marti, C. Briones, E. Roman, E. Briand, C. M. Pradier and J. A. Martin-Gago, *Langmuir*, 2005, **21**, 9510–9517.
21 W. Liao, F. Wei, D. Liu, M. X. Qian, G. Yuana and X. S. Zhaoa, *Sens. Actuators, B*, 2006, **114**, 445–450.
22 J. Park, D. Bang, K. Jang, E. Kim, S. Haam and S. Na, *Nat. Commun.*, 2014, **5**, 3456.

